ELSEVIER

Thermochimica Acta 388 (2002) 21–25

thermochimica acta

www.elsevier.com/locate/tca

Effect of water vapor pressure on thermal dehydration of lithium sulfate monohydrate

Yasuyoshi Seto[a], Hisanari Sato[b], Yoshio Masuda[c,*]

[a]*Graduate School of Science and Technology, Niigata University, Niigata 950-2181, Japan*
[b]*Department of Chemistry, Faculty of Science, Niigata University, Niigata 950-2181, Japan*
[c]*Department of Environmental Science, Faculty of Science, Niigata University, Niigata 950-2181, Japan*

Received 1 June 2001; received in revised form 2 August 2001; accepted 2 August 2001

Abstract

The effect of the atmospheric water vapor pressure on the rate of thermal dehyration of lithium sulfate monohydrate was studied by means of isothermal gravimetry under various water vapor pressures, ranging from 0 to 2666 Pa. The kinetics of dehydration was described by the two-dimensional Arvada–Erofe'ev type equation, $A_2(\alpha)$. An unusual dependence of the rate of dehydration on the atmospheric water vapor pressure was observed as follows. At high temperature, the rate constant increased with increasing water vapor pressure, reached a maximum and decreased gradually to a constant value. At low temperatures, 90 and 100 °C, the rate constants decreased at first, passed through minimum, increased and then decreased. These unusual phenomena are known as the Smith–Topley effects. The mechanism of the phenomena can be discussed on the basis of the diffusion process of the dehydrated water molecules through the product phase.

Keywords: Thermal dehydration; Effect of atmospheric water vapor pressure; Smith–Topley effect; Isothermal gravimetry

1. Introduction

The thermal dehydrations of solid hydrates have been studied extensively by means of thermal analyses such as the thermogravimetry (TG), differential thermal analysis (DTA) and differential scanning calorimetry (DSC). It has been known that the dehydrations of hydrates are generally reversible and influenced by the effect of the product phase on the ease of water escape, because such residual product tends to greater or lesser extent diminish the rate of diffusion of water from the reaction interface.

Smith and Topley reported that the rate constants for the dehydration of manganese(II) oxalate dihydrate and copper(II) sulfate pentahydrate varied unusually with the partial pressure of atmospheric water vapor. As the water vapor pressure increased, the rate of dehydration initially decreased, then passed through a minimum, increased strongly to a maximum, and finally decreased more slowly [1,2]. This unusual phenomenon is known as the Smith–Topley effect. Recently, similar phenomena have been also observed in dehydration of the other hydrates [3–6]. The effect, however, has not been always recognized in all dehydrations. The authors found similar phenomena to the Smith–Topley effect and pointed out that the effect could be related to the crystallinity of the dehydrated products [7–10].

* Corresponding author.
E-mail address: masuda@sc.niigata-u.ac.jp (Y. Masuda).

0040-6031/02/$ – see front matter
PII: S0040-6031(02)00049-7

In the present study, the Smith–Topley effect can be also observed for the thermal dehydration of lithium sulfate monohydrate, and the mechanism of the phenomenon is discussed briefly on the basis of the crystallinity of the dehydration product and the transfer of the dehydrated water molecules from the reaction interface.

2. Experimental

Lithium sulfate monohydrate was purchased from Wako Pure Chemical Ind. Ltd., Osaka. The guaranteed reagent was re-crystallized from distilled water and the polycrystalline sample was obtained. The specimen was identified by means of TG and IR spectra. The crystals were pulverized with a pestle in a mortar, and sieved to a narrow fractions of 100–150 mesh size.

The isothermal dehydration was followed with a Shinku–Riko TGD 5000RH differential microbalance equipped with a gold image furnace [7–11]. About 6 mg sample was weighed into platinum crucible and set in the microbalance. The furnace was maintained at a constant temperature within ±0.5°, until the dehydration was completed. The output voltages for the mass loss from the microbalance were amplified and acquired on a microcomputer, Epson 286 via an A/D converter (Datel–Intersil 7109 modified to 13 bit) [7–11]. For each dehydration process, about 1000 data points relating to the mass loss were collected at given time intervals, and the fraction of dehydration, α, was calculated from the data.

All dehydrations were carried out at an atmospheric water vapor pressure and controlled partial pressures of water vapor, P_{H_2O}. The P_{H_2O} of the reaction system was controlled as follows [11]. Nitrogen gas was bubbled into boiling water, the gas was passed through a condenser controlled at a constant temperature to obtain a constant vapor pressure, and then the gas (flow rate 60 $cm^3\ min^{-1}$) was admitted to the microbalance.

The X-ray powder diffraction profiles were obtained with a Geigerflex RAD-R diffractometer with a high-temperature sample holder. Cu Kα radiation, a nickel filter and a graphite monochrometer were used in all measurements. The diffraction data were taken at steps of width 0.02°. IR spectra were measured from 250 to 4000 cm^{-1} in a KBr disk with a Hitachi 295 spectrophotometer.

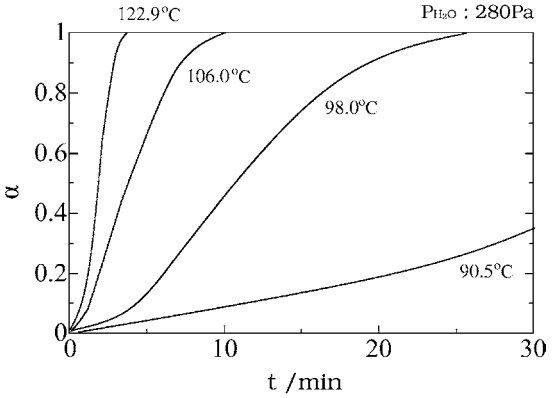

Fig. 1. Typical plots of dehydration fraction, α vs. reaction time, t at water vapor pressure of 280 Pa.

3. Results and discussion

The smoothness of the TG and DTA curves of the sample and the agreement between the calculated and observed weight loss suggest that the dehydration proceed successively without any intermediate. Fig. 1 shows a typical plot of the dehydration fraction, α against the reaction time, t. Kinetics of the dehydration were analyzed by means of integral method as follows. The rate of dehydration can be expressed by

$$\frac{da}{dt} = kf(\alpha) \tag{1}$$

where, α is the dehydration fraction after time of t, k the rate constant, and $f(\alpha)$ is a function depending on the dehydration mechanism and geometry of the reacting particles. Many theoretical model functions have been proposed for $f(\alpha)$ [12–16]. The Eq. (1) can be converted to the integrated form

$$G(\alpha) \equiv \int \frac{da}{f(\alpha)} = \int k\,dt = kt \tag{2}$$

where, $G(\alpha)$ is the function depending on the dehydration mechanism as well as $f(\alpha)$. The $G(\alpha)$ of the present dehydration was determined by the linearity of the plot of various $G(\alpha)$ against t, in accordance with Eq. (2).

Fig. 2 shows the the plot of $G(\alpha)$ against t for the isothermal dehydration of $Li_2SO_4{\cdot}H_2O$ at the atmospheric water pressure of 1333 Pa. Authors examined

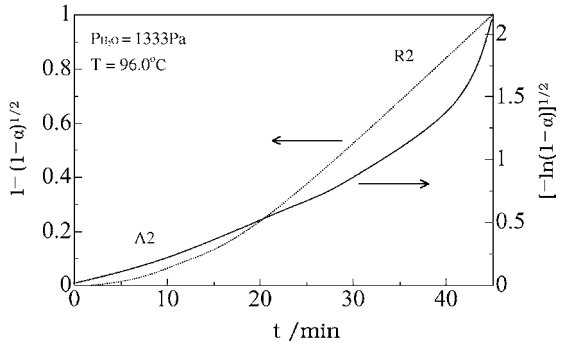

Fig. 2. Typical plots of $G(\alpha)$ vs. t at water vapor pressure of 1333 Pa.

plots for the various models of $G(\alpha)$. The plot according to the equation

$$[-\ln(1-\alpha)]^{1/2} = kt \quad (3)$$

shows the best linearity over the first half of dehydration. This equation is referred to as the two-dimensional Avrami–Erofe'ev equation $A_2(\alpha)$ [17–20]. The best model function for the second half of the dehydration can be described as the two-dimensional phase boundary reaction $R_2(\alpha)$,

$$1-(1-\alpha)^{1/2} = kt \quad (4)$$

The $A_2(\alpha)$ equation is the kinetic expression concerned with the random nucleation and nuclei growth process.

A convenient explanation of this result will be put forward as follows. In the initial stage of dehydration, the nuclei are formed on the surface of the specimens. When a great number of nuclei grow and cover the surface of the reacts, an interface is built up between the hydrated and dehydrated salt, and the interface advances from the surface to inward of the specimen at the constant rate. Therefore, the present dehydration looks apparently like a two-dimensional phase boundary reaction $R_2(\alpha)$ in their second half.

Table 1 shows the variation of $G(\alpha)$ from $A_2(\alpha)$ to $R_2(\alpha)$ at various temperatures and water vapor pressures. At low temperatures the dehydration is described by the $A_2(\alpha)$ model function at initial range of α, however, at higher temperature ranges the dehydration can be described only by the $A_2(\alpha)$ function. Therefore, the authors discuss, hereafter, the relation ship between the rate constant, k of $A_2(\alpha)$ and the atmospheric water vapor pressure.

Table 1
Variation of $G(\alpha)$ with the atmospheric water vapor pressure and temperature

P_{H_2O} (Pa)	T (°C)	G (α)	Range of α	ln k
280	90	A_2	0.01–0.54	−7.96
		R_2	0.53–1.00	−8.22
	100	A_2	0.01–0.61	−6.76
		R_2	0.54–0.93	−7.09
	110	A_2	0.09–0.89	−5.70
		R_2	0.47–0.99	−6.11
	120	A_2	0.19–0.86	−4.95
		R_2	0.38–0.99	−5.62
667	90	A_2	0.02–0.59	−7.32
		R_2	0.58–1.00	−7.66
	100	A_2	0.06–0.79	−6.09
		R_2	0.45–1.00	−6.59
	110	A_2	0.09–0.82	−5.49
		R_2	0.43–0.98	−6.01
	120	A_2	0.01–0.85	−4.74
		R_2	0.62–1.00	−5.16
1333	90	A_2	0.00–0.54	−7.88
		R_2	0.55–1.00	−8.20
	100	A_2	0.00–0.65	−6.72
		R_2	0.54–1.00	−7.06
	110	A_2	0.14–0.78	−5.82
		R_2	0.52–1.00	−6.33
	120	A_2	0.11–0.81	−4.97
		R_2	0.58–1.00	−5.40
2066	90	A_2	0.00–0.42	−8.28
		R_2	0.55–1.00	−8.60
	100	A_2	0.00–0.69	−7.21
		R_2	0.49–1.00	−7.58
	110	A_2	0.00–0.75	−6.00
		R_2	0.62–1.00	−6.46
	120	A_2	0.06–0.85	−4.99
		R_2	0.52–1.00	−5.49
2680	90	A_2	0.00–0.50	−8.55
		R_2	0.40–1.00	−8.94
	100	A_2	0.00–0.40	−7.49
		R_2	0.54–1.00	−7.89
	110	A_2	0.09–0.82	−5.77
		R_2	0.50–0.99	−6.24
	120	A_2	0.05–0.90	−5.03
		R_2	0.52–1.00	−5.54

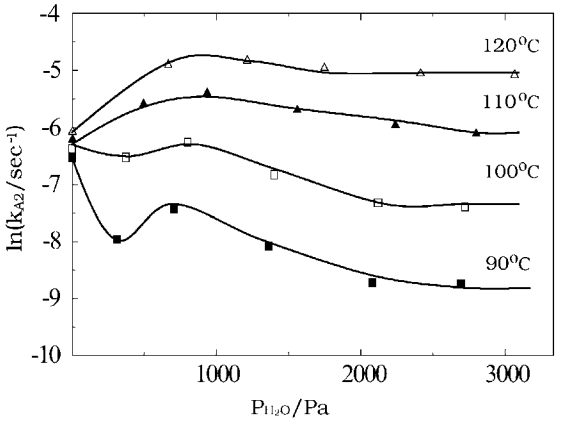

Fig. 3. Variation of dehydration rate, k_{A_2} with various atmospheric water vapor pressures.

Fig. 3 shows the relation ship between the rate of dehydration, k and the water vapor pressure at particular temperatures. At high temperature, the value of k increased with increasing of the water vapor pressure, reached to a maximum and decreased gradually to a constant value. At low temperatures as 90 and 100 °C, the rate constants decreased at first, passed through minimum, increased and then decreased gradually to a constant value. This unusual phenomenon is known as the Smith–Topley effect.

Recently, the authors found similar phenomena for the dehydrations of zinc formate dihydrate, erbium formate dihydrate and yttrium formate dihydrate [7–9]. They discussed the mechanism of the unusual phenomena in correlation of the crystallinity of the dehydration products [21], and found that the crystallinity of dehydration products was affected by the experimental temperature and the water vapor pressure and the presence of a few water molecule promoted the crystallization of the dehydrated products. Namely, at a low water vapor pressure, the amorphous dehydrated product covers the reaction particles and the dissociated water molecules may be adsorbed by the narrow walls of molecular dimensioned capillaries in the produced phase. These findings would interfere with escape of further water molecules and the rate must be inhibited. Because water molecules promote the crystallization of anhydride product at higher water vapor pressure, the crystallization forms wide channels among the dehydrated product, through which the dehydrated water molecules escape easily. So the rate constant would increase at higher water vapor pressures.

In the present dehydration, the authors could not detect the amorphous anhydride by the X-ray diffraction profile measured immediately after the dehydration even in vacuo. However, the possibility of the formation of amorphous anhydride products is undeniable. Because the amorphous phase formed may be so unstable that it crystallize quickly, the unstable amorphous phase could not be recognized in the time resolution of the X-ray diffraction measurement.

The results obtained at low water vapor pressure (less than 666 Pa) especially at low temperatures of 90 and 100 °C, suggested the formation of an unstable amorphous anhydride. Namely, the unstable amorphous anhydride adsorbed the dissociated water molecules and the dehydration rate may be restrained at these water vapor pressures and temperatures. Because of the crystallinity of the anhydrous product promoted at the regions of higher temperatures and higher water vapor pressures, the rate constant would increase with increasing water vapor pressure and temperature. At the regions of higher water vapor pressure than 1333 Pa, the apparent rate of dehydration decreased gradually due to the reverse reaction.

The equation $A_2(\alpha)$ is the kinetic expression concerned with the random nucleation and nuclei growth. Hulbert pointed out the relationship between the nuclei growth and diffusion process of migrating species as follows [13]. When (i) the nucleation rate is assumed to be constant, (ii) the nuclei grow two-dimensionally and (iii) the growth is diffusion controlled, the Eq. (3) can be derived on the basis of the overall rate constant to be given by Eq. (5)

$$k = \left(\frac{\pi hID}{2}\right)^{1/2} \tag{5}$$

where, I is the nucleation rate per unit volume, h the thickness of the sample, and D is the diffusion coefficient of the migrating species. On the basis of above opinion, the reaction described by the $A_2(\alpha)$ would be controlled by the diffusion process of the migrating species, i.e. in the present dehydration, the rate would be controlled by the diffusion on the dissociated water molecules through the phase.

Fig. 4 shows the Arrhenius plots at various water vapor pressures. The values of activation energy, E and the frequency factor, A are shown in Table 2. These values are compatible to those reported for the dehydration of lithium sulfate monohydrate in a flow of

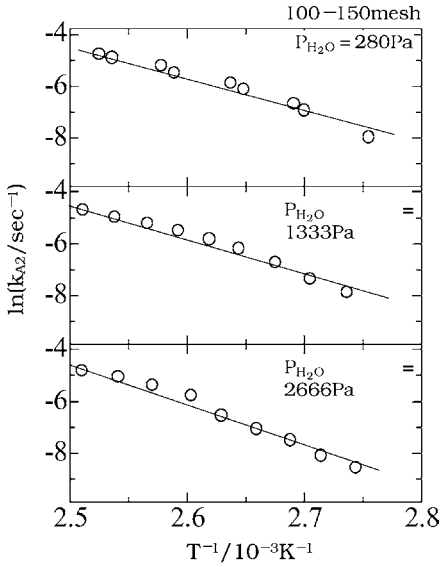

Fig. 4. Arrhenius plots of k_{A_2} measured at various atmospheric water vapor pressures.

Table 2
Activation energy (E) and frequency factor (A) for the dehydration of lithium sulfate monohydrate

P_{H_2O} (Pa)	E (kJ mol^{-1})	A (s^{-1})
280	110.3	3.54×10^{12}
1333	117.8	3.17×10^{13}
2666	140.9	3.30×10^{16}

nitrogen [22], however, the values of E are considerably higher than those reported for the dehydration in vacuo (22.1–29.3 kJ mol^{-1}), and the dehydration rates are slower than those in vacuo [23]. In the present case, the dehydration is controlled by the diffusion on the dissociated water molecules, therefore, the rate must be dependent on the difference of the partial water vapor pressure in the surrounding. Thus, the slow rate of the present dehydration may be explained on the above basis. It is worth noting that the values of E increased with increasing atmospheric water vapor pressure. This finding shows that the presence of atmospheric water molecules has an enormous influence on the rate of the dehydration.

In general [24–26], the magnitude of A for the thermal decomposition is expected to be $\sim 10^{13}$ s^{-1}, which is comparable to a frequency of vibration in the crystal lattice. The values of A for the present dehydration at 2666 Pa is larger than that expected by factors 10^3. Shannon [26] has discussed the values of A for several reactions, and pointed out that the large value of A for the dehydration was attributable to adsorption of the mobile water molecules on the reaction interface. Therefore, it is likely for the present dehydration that the dissociated water molecules are adsorbed on the reaction interface and influence the rate of dehydration [11]. The equilibrium water vapor pressure for the present dehydration has not been measured, however, a reverse reaction appears to occur at high water vapor pressures and the apparent rate is hindered by atmospheric water molecules.

References

[1] M.L. Smith, B. Topley, Proc. R. Soc. Ser. A 134 (1931) 224.
[2] B. Topley, M.L. Smith, J. Chem. Soc. (1935) 321.
[3] W.E. Garner, M.G. Tanner, J. Chem. Soc. (1930) 47.
[4] W.E. Garner, T.S. Jennings, Proc. R. Soc. Ser. A 224 (1954) 460.
[5] D. Dollimore, T.E. Jones, P. Spooner, J. Chem. Soc. A. (1970) 2809.
[6] D. Dollimore, G.R. Heal, J. Mason, Thermochim. Acta 24 (1978) 307.
[7] Y. Masuda, K. Nagagata, Thermochim. Acta 155 (1989) 255.
[8] Y. Masuda, K. Hirata, Y. Ito, Thermochim. Acta 203 (1992) 289.
[9] Y. Masuda, Y. Ito, J. Therm. Anal. 38 (1992) 1793.
[10] Y. Masuda, K. Iwata, R. Ito, Y. Ito, J. Phys. Chem. 91 (1987) 6543.
[11] Y. Masuda, K. Iwata, J. Therm. Anal. 44 (1995) 1013.
[12] J.H. Sharp, G.W. Brindley, B.N.N. Achar, J. Am. Ceram. Soc. 49 (1966) 379.
[13] S.F. Hulbert, J. Br. Ceram. Soc. 6 (1969) 11.
[14] J. Sestak, G. Berggen, Thermochim. Acta 3 (1971) 1.
[15] K. Heide, W. Holand, H. Golker, K. Seyfarth, B. Muller, R. Sauer, Thermochim. Acta 13 (1975) 365.
[16] W.E. Brown, D. Dollimore, A.K. Gallway, in: C.H. Bamford, C.F.H. Tipper (Eds.), Comprehensive Chemical Kinetics, Reactions in Solid State, Vol. 22, Elsevier, Amsterdam, 1980, p. 90.
[17] M. Avrami, J. Chem. Phys. 7 (1939) 1103.
[18] M. Avrami, J. Chem. Phys. 8 (1940) 212.
[19] M. Avrami, J. Chem. Phys. 9 (1941) 177.
[20] B.V. Erofe'ev, C.R. (Dokl.) Acad. Sci. USSR 52 (1946) 511.
[21] Y. Masuda, Netu Sokutei 22 (1995) 203.
[22] N. Koga, H. Tanaka, J. Phys. Chem. 93 (19989) 7793.
[23] Y. Masuda, H. Takeuchi, A. Yahata, Thermochim. Acta 228 (1993) 191.
[24] W.E. Brown, D. Dollimore, A.K. Gallway, in: C.H. Bamford, C.F.H. Tipper (Eds.), Comprehensive Chemical Kinetics, Reactions in Solid State, Vol. 22, Elsevier, Amsterdam, 1980, p. 123.
[25] M. Polany, E. Wigner, Z. Phys. Chem. Abstr. A 139 (1928) 92.
[26] R.D. Shannon, Trans. Faraday Soc. 60 (1964) 1902.